Bis(quercetinato)oxovanadium IV Reverses Metabolic Changes in Streptozotocin-Induced Diabetic Mice

Ruchi Shukla[1], Subhash Padhye[2], Manisha Modak[3],
Saroj S. Ghaskadbi[3] and Ramesh R. Bhonde[1]

[1] *Tissue Engineering and Banking Laboratory, National Centre for Cell Science, Pune University Campus, Ganeshkind, Pune 411007, India.* [2] *Department of Chemistry, University of Pune, Pune, India.* [3] *Department of Zoology, University of Pune, Pune, India. Address correspondence to: Ramesh R. Bhonde, e-mail: rrbhonde@nccs.res.in*

■ Abstract

Organic vanadium compounds offer several advantages in the treatment of diabetes, yet they are impractical to use because of known side effects. In order to ameliorate the side effects of vanadium, we conjugated it with quercetin to form bis(quercetinato)oxovanadium IV (BQOV). This study evaluates the effect of BQOV treatment on carbohydrate metabolism and overall oxidative stress in streptozotocin-induced (STZ) diabetic mice. Administration of BQOV orally to diabetic mice for 3 weeks led to a reduction of blood glucose levels and the animals exhibited normal glucose tolerance at the end of the study period. The increase in glucose uptake by skeletal muscle and liver as well as the normalization of mRNA levels of G-6-Pase and glucokinase in the liver after BQOV treatment pointed to improvements in carbohydrate metabolism. The analysis of the antioxidant status of serum, liver and pancreas revealed reduced oxidative stress in BQOV-treated animals compared to untreated diabetic controls. Serum analyses for kidney and liver function showed that BQOV treatment provoked total protection of the kidney and partial protection of the liver from diabetogenic insults. The number of insulin-positive cells and the amount of pancreatic insulin in treated mice (1.2038 ± 0.34 ng/mg tissue) did not account for pancreatic regeneration but suggested an insulin-mimetic action on the part of BQOV. Moreover, administration of BQOV for 3 weeks did not show any visible side-effects. This data indicate that BQOV is a safe and potent agent for diabetes treatment, because it is able to improve carbohydrate metabolism and to reduce overall oxidative stress.

Keywords: vanadium · pancreatic regeneration · insulin mimetic · oxidative stress · glucokinase and G-6-Pase

Introduction

Type 2 diabetes mellitus is a metabolic disorder caused by insufficient insulin production leading to hyperglycemia as a result of a reduced glucose uptake by the peripheral tissues and increased gluconeogenesis [1]. While designing a treatment regime for a diabetes patient, the primary target is tight glycemic control. Because of sustained hyperglycemia, there is increased free radical generation leading to secondary complications like nephropathy, retinopathy and cardiomyopathy caused by damage to cellular proteins, membrane lipids, and nucleic acids, which eventually leads to cell death mainly through activation of poly(ADP-ribose) polymerase-1 [2, 3].

Vanadium compounds are well documented as potential anti-diabetic agents [4]. Vanadium has been shown to reduce blood glucose by normalizing the expression of key carbohydrate metabolic enzymes like phosphoenolpyruvate carboxykinase (PEPCK) and

glucose-6-phosphatase (G-6-Pase) in the liver and kidney [5]. Moreover, it has been shown to normalize the expression of GLUT4 in muscles, thus increasing peripheral glucose uptake [6]. However, these vanadium compounds are not free from side effects and are generally associated with diarrhea and GI tract abnormalities [7]. Recently, Scior *et al.* critically reviewed the question of the drugability of vanadium compounds and concluded that vanadium is a drugable agent. It is, however, essential to develop more potent vanadium compounds with higher efficacy and reduced side effects [8]. Vanadium efficacy can be increased by synthesis of organic vanadium chelates. Yuen *et al.* studied the glucose lowering effect of $VOSO_4$ and bis(maltolato)oxovanadium IV (BMOV) on streptozotocin-diabetic (STZ-diabetic) animals and found BMOV to be 2 to 3 times more potent than $VOSO_4$ [9]. Several other studies have supported the idea that conjugation of vanadium with an organic moiety increases its efficacy and decreases side-effects. However, concerns about vanadium toxicity are always present [10]. Reul *et al.* have shown the increased efficacy and reduced toxicity of the organic vanadium compounds in comparison to inorganic vanadium salt, $VOSO_4$ [11].

In an effort to increase gastrointestinal absorption and reduce the toxicity of vanadium we have conjugated a flavonoid, quercetin with vanadium and synthesized BQOV [12]. The conjugate has immense hypoglycemic potential and has been found to be much less toxic than the parent vanadium salt in both *in vitro* and *in vivo* studies [13]. The present study examines the effect of long term administration (3 weeks) of BQOV on glycemic status, carbohydrate metabolism, overall oxidative stress and pancreatic regeneration in STZ-induced diabetic Balb/c mice. We have explored the mechanism of action of the conjugate and the dominant partner of vanadium and quercetin in the context of various activities of BQOV, since vanadium and quercetin are known to have antagonistic effects.

Materials and methods

Materials

Streptozotocin, tri-reagent, primers, quercetin, ABTS, DPPH, ethedium bromide, hematoxylin, eosin, DMEM and FCS were obtained from Sigma-Aldrich Reagents (St. Luis, MO, USA), 2-NBDG from Molecular Probes Corp. (Eugene Oregon, USA), BCA kit from Pierce Biotechnology Inc. (Rockford, IL, USA), RNAlater, Platinum Taq and agarose from Invitrogen

Corp. (Carlsbad, CA, USA) and mounting antifade media from Oncogene Research Products (San Diego, Calfornia, USA).

Treatment with BQOV

6-8 week old, male Balb/c mice were obtained from the animal facility of the National Centre for Cell Science, Pune, India. The animals were made diabetic by injecting streptozotocin (STZ) at a dose of 180 mg/kg intraperitoneally. The animals were kept for one week to develop hyperglycemia. Blood glucose was checked using an automated glucose analyzer (Accu-Check Sensor Comfort, Roche Diagnostics GmbH, Mannheim, Germany) and blood was obtained by the tail nick method. Animals with a fasting blood glucose above 200 mg/dl were included in the study as diabetics. Diabetic animals were randomly divided into three groups of 5-8 animals. The first group was administered daily oral doses of BQOV (0.2 mmol/kg) once in the morning between 10:00-11:00, the second group was administered oral doses of the vehicle, DMSO (0.5 ml/kg, 10% in water), for 3 weeks and the third set was kept as untreated diabetic controls. At the same time, age and sex matched normal Balb/c mice were also kept under similar conditions to act as normal untreated controls. Body weight and blood glucose levels were measured every 7th day without fasting, just before that day's administration of the drug. During the whole experimentation period, the mice were kept under controlled conditions (22 ± 2°C) with 12 h light and dark cycles and had free access to water and feed. All animal experiments were performed according to the guidelines approved by the Committee for the Purpose of Control and Supervision of Experiments on Animals (Government of India) and with the permission of the institute's animal care and use committee.

OGTT and glucose uptake by liver and muscles

At the end of the study period animals were kept fasting for 10 hours and glucose (2 g/kg) was administered orally. Blood glucose was determined prior to (0 min) and then 30 min, 60 min and 90 min after glucose ingestion. In another set of animals, 2-NBDG (0.05 mmol/kg) was injected intravenously into the animals at the 30-min time point of the OGTT and the animals were killed at the 60-min time point to collect muscle and liver biopsies. The tissue sections (10-15 μm) were cut using cryotome and mounted with antifade mounting medium (Oncogene) containing DAPI. The slides were observed under an LSM510 confocal microscope

(Carl-Zeiss, Germany) at excitation/emission wavelength of 465/540 nm for visualization of 2-NBDG and UV excitation for DAPI. Images were captured by the CCD-4230 camera coupled with the microscope and processed using the computer-based programmable image analyzer KS300. A semi-quantitative analysis (2.5D) of 2-NBDG intensity was performed using LSM5 image examiner software.

Glucose uptake by L6 myoblasts

L6 cells were procured from the Cell Repository of the National Centre for Cell Science, Pune, India and regularly marinated in DMEM with 10% FCS. 20-24 h serum-starved cells were incubated in glucose free media for 30 minutes and treated with 25 µM BQOV or 100nM insulin. 300 µM fluorescence-labeled glucose, 2-NBDG (2-(N-(7-nitrobenz-2-oxa-1,3-diazol-4-yl) amino)-2-deoxyglucose) was then added to the medium and cells were incubated for another 15 minutes. The medium was then changed to 2-NBDG free media and cells were incubated for another 5 minutes before being washed a final time with chilled PBS and fixed with 4% paraformaldehyde. The cells were then mounted with an antifade mounting media for observation under the fluorescence microscope.

RNA extraction

The liver was excised and immersed in RNAlater (Invitrogen) and stored at -85ºC until RNA isolation. Total cellular RNA was extracted from the excised liver tissues using Tri-Reagent (Sigma), according to the manufacturer's instructions. About 100 mg of tissue was homogenized for a short time in 1 ml reagent and RNA was extracted from the homogenates by adding chloroform (1 vol homogenate +0.1 vol. chloroform). After 10 min the suspensions were centrifuged at 12,000 x g (4ºC, 15 min). The RNA was precipitated from the aqueous phase by addition of an equal volume of isopropanol. Samples were incubated for 15 min and centrifuged at 12,000 x g (4ºC, 10 min). The supernatant was removed and the RNA was washed once with 70% ethanol and centrifuged at 12,000 x g (4ºC, 5 min). After removing the supernatant, the RNA pellet was dried briefly and dissolved in 50 µl diethylpyrocarbonate (DEPC)-treated distilled water. RNA was quantified by measuring absorbance spectrophotometrically at 260 nm.

RT-PCR of G-6-Pase and glucokinase

Reverse transcription of 5 µg total RNA was performed using the Reverse Transcription System (Promega) according to the manufacturer's instructions. The cDNA thus formed was used for PCR reactions. The PCR mixture contained 250 µM dNTP, 1.5 mM MgCl$_2$, 0.5 U Platinum Taq DNA polymerase (Invitrogen), 1 µl sense and antisense primers, 5 µl RT product, and 2.5 µl 10X Taq buffer (Invitrogen). The reaction mixtures were subjected to 25 cycles of PCR amplification consisting of denaturation for 60 sec at 94ºC, annealing for 60 sec at 55ºC or 58ºC and elongation for 60 sec at 72ºC. The final extension was completed at 72ºC for 7 min. The oligonucleotide primers used were: (5'-TAAGTGGATTCTTTTTGGACA-3' sense and 5'-GAAGAGGCTGGCAAAGGGTGT-3' antisense) for G-6-Pase at 55ºC, which amplified a 562-bp cDNA and primer set (5'- CACCCAACT GCGAAATCACC-3' sense and 5'-CATTTGTGG GGTGTGGAGTC-3' antisense) for glucokinase at 58ºC, which amplified a 161-bp cDNA. G-6-Pase and glucokinase mRNA expression levels were normalized to β-actin RNA expression using the primer set (5'-TGGAATCCTGTGGCATCCA-3' sense and 5'-TAACAGTCCGCCTAGAAGCA-3' antisense) at

Table 1. Blood glucose and body weight profile of animals

Mice	Blood glucose (in mg/dl)				Body weight (in g)			
	Initial	Week 1	Week 2	Week 3	Initial	Week 1	Week 2	Week 3
Normal	88.75 ± 10.5	92.5 ± 6.4	110.0 ± 4.5	83.55 ± 12.5	22.0 ± 2.0	22.0 ± 3.5	24.0 ± 2.0	25.0 ± 3.0
Diabetic (treated)	467.50 ± 56.8	291.3 ± 56.2	276.0 ± 73.7	168.70 ± 40.7	18.0 ± 2.5	18.0 ± 2.0	20.0 ± 2.0	22.0 ± 2.5
Diabetic (untreated)	409.00 ± 57.2	423.0 ± 74.5	470.6 ± 94.2	437.40 ± 115.3	18.0 ± 2.0	18.0 ± 3.0	16.0 ± 2.5	16.0 ± 2.0
Diabetic (vehicle)	430.00 ± 42.5	462.5 ± 90.3	438.5 ± 60.5	445.40 ± 80.7	19.0 ± 3.0	18.0 ± 2.5	17.0 ± 4.0	18.0 ± 2.0

Legend: The table represents non-fasting blood glucose levels in normal, treated diabetic, untreated diabetic and vehicle-administered diabetic animals during the study period. Values are expressed in mg/dl and represent mean ± SD (n = 8-10).

58°C, which amplified 315-bp cDNA. 3 μl 10X loading buffer (Invitrogen) was added to the PCR samples and 15 μl of PCR products were electrophoresed on 1.5 % agarose gel stained with ethidium bromide. The gels were photographed under UV light. The intensity of the mRNA bands was analyzed by densitometry using GeneTools software from SynGene.
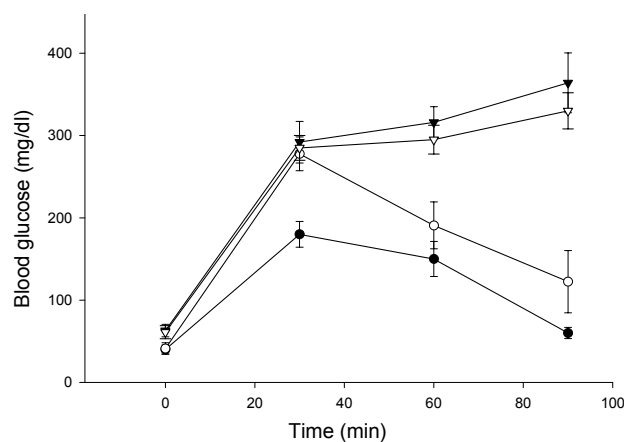

Figure 1. Oral glucose tolerance curve. Animals in all four groups (normal -●-; BQOV-treated -○-; untreated diabetic -▼-; vehicle-administered -▽-) were kept for 10 hours fasting and then glucose (2 g/kg) was administered orally. Blood glucose was monitored at 30 min intervals till 90 min. Values represent mean ± SD (n = 5).

Serum analysis

At the end of the study period, serum was collected and its antioxidant status was assessed using three different methods, including two based on the measurement of free radical scavenging activity: 2.2'-azinobis(3-ethylbenzothiazoline-6-sulfonic acid) diammonium salt (ABTS) assay [14] and 2,2-diphenyl-picrylhydrazyl (DPPH) assay [15]. Trolox was taken as standard and results were expressed as mM trolox equivalents. The third method was based on the reduction of a ferric tripyridyl-s-triazine complex to its ferrous form, namely ferric reducing antioxidant power (FRAP) assay, as described by Benzie and Strain [16] and the results were expressed as quercetin equivalents (QE). Furthermore, urea, creatinine and alkaline phosphatase levels were measured using standard biochemical assays.

Histopathology of liver and kidney

Tissues were excised, washed once in PBS and then fixed in formalin (10%). Tissues were then processed for paraffin embedding and subsequent serial sectioning. The sections were deparaffinized by two washes of xylene (5 min each), passed through an alcohol grade and rehydrated. The sections were then stained with hematoxylin/eosin to enable the histological changes to be assessed.

Antioxidant enzyme activities in liver and pancreas

The tissues were homogenized in phosphate buffer and the homogenate was used to measure the activity of the antioxidant enzymes viz. catalase, superoxide dismutase (SOD) and glutathione peroxidase (GPX) using standard spectrophotometric assays. Briefly, catalase activity in the tissue homogenate was determined spectrophotometrically by checking the rate of H_2O_2 degradation at 240nm in presence of the homogenate [17]. SOD assay was carried out by generating superoxide radicals by the photochemical reduction of flavins, which reduces NBT into a blue-colored compound, formazone. SOD quenches free oxygen radicals and inhibits reduction of NBT, which can be measured at 560nm [18]. GPx catalyzes the reduction of various organic hydroperoxides, as well as that of hydrogen peroxide with glutathion as hydrogen donor. The reaction can be monitored spectrophotometrically at 340nm [19]. The amount of protein in the homogenate was determined by BCA method and enzyme activity is reported in terms of U/mg protein.

Lipid peroxidation level in liver and pancreas

Lipid peroxidation is a good way of evaluating oxidative stress-induced damage to tissues. Hence the amount of lipid peroxidation was determined in terms of malonyldialdehydes (MDA) formed per mg protein of tissue. Briefly, 0.8% TBA (1.5 ml), 8.1% SDS (200 μl), 20% acetic acid (1.5 ml) and distilled water (600 μl) were added to 200 μl tissue homogenate. The entire reaction mixture was kept at 90°C for 45 minutes and immediately cooled on ice. The pink color representative of thiobarbituric acid reactive substances was measured at 532 nm [20].

Immunofluorescence staining of pancreatic sections

Pancreatic sections were fixed in 10% buffered formalin and embedded in paraffin. Tissue sections (10μm) were cut using a microtome blade. The sections were deparaffinized, passed through alcohol grades (90%, 70%, 50%, 30%, water) and hydrated for immunostaining. The sections were incubated with guinea pig anti-insulin (Linco Research Inc., St.
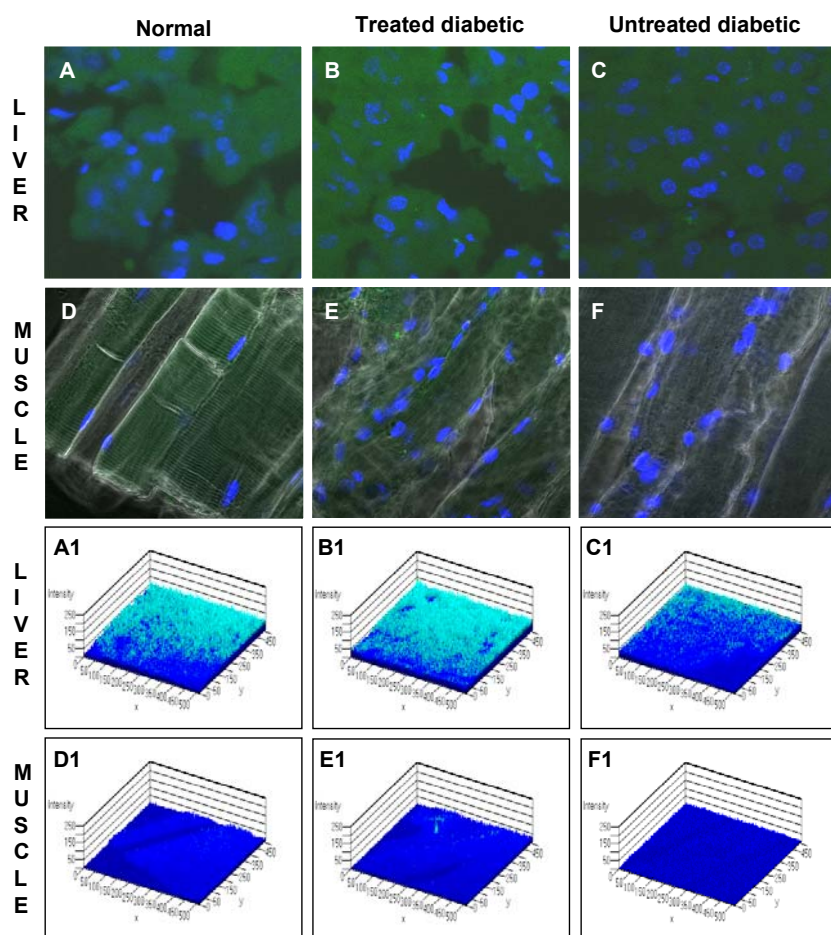
Figure 2. Glucose uptake in liver and skeletal muscle. During OGTT, animals were injected with 2-NBDG at the 30 min time point and then sacrificed after 30 min to collect liver and muscle. Cryosections (10µm) were cut and observed under a confocal microscope at 485/540 nm wavelength to observe green fluorescence of 2-NBDG and UV in order to locate the DAPI stained nucleus. The upper row of images shows liver sections of normal, treated diabetic and untreated diabetic groups respectively (**A**-**C**). The second row of images shows muscle sections of normal, treated diabetic and untreated diabetic groups respectively (**D**-**F**). The lower panel shows 2.5D analysis images of the sections respectively, where the x and y axis are the pixels and the z axis represents intensity depicting the semi-quantitative uptake of 2-NBDG (**A1**-**F1**).

Pancreatic insulin content

Pancreas were excised and weighed. The tissue was homogenized in acid ethanol by mincing and sonication. The amount of insulin was quantitated using a mouse-insulin ELISA kit (Mercodia). The results were expressed in terms of nanogram insulin per mg tissue.

Statistical analysis

Values are expressed as mean ± S.D. and n = number of mice in each group. Statistical analyses were performed using one-way ANOVA followed by Tukey test using SigmaStat, version 2.03. $p < 0.05$ was taken as significance level.

Results

Blood glucose profile, OGTT and body weight

Table 1 depicts blood glucose levels in untreated and treated diabetic animals. A significant decrease in random blood glucose level in BQOV-treated diabetic animals was observed, while untreated animals exhibited sustained hyperglycemia. A gradual decrease in random blood glucose was observed in the BQOV-treated group that approached normal levels at the end of the study period. There was no reduction in the blood glucose levels of vehicle-administered animals,

Charles, Missouri, USA) and mouse anti-glucagon primary (Sigma-Aldrich Reagents, St. Luis, MO, USA) antibodies. Alexa Flour 488 goat anti-guinea pig IgG and Alexa Flour 546 goat anti-mouse IgG from Molecular Probes (Eugene, Oregon, USA) were used as secondary antibodies to detect insulin- and glucagon-positive cells respectively. The tissue sections were finally mounted with antifade mounting media containing DAPI. The slides were observed under an LSM510 confocal microscope (Carl-Zeiss, Jena, Germany).

thus emphasizing the effect of BQOV on blood glucose levels. However, the treatment had no marked effect on the animals' body weight. Although BQOV administration had prevented further loss of weight, it was unable to increase body weight significantly. Moreover, the OGTT curve of the treated-diabetic animals was comparable to that of the normal animals, whereas untreated diabetic animals exhibited an abnormal OGTT (Figure 1). A rise in blood glucose levels 30 min after glucose administration was observed in

all the groups. However, further glucose clearance was observed only in normal and BQOV-treated animals, while the untreated and vehicle-administered animals exhibited no glucose clearance from the blood.

Peripheral glucose uptake

Figure 2 depicts 2-NBDG incorporation into the liver and muscles of the animals. Treated animals exhibited fluorescence comparable to those of normal animals, whereas there was very little fluorescence in the liver and muscles of untreated animals, indicating increased glucose uptake in the liver and skeletal muscles of BQOV treated animals as compared to the untreated diabetic group.

In vitro glucose uptake potential of BQOV

Figure 3 represents fluorescence images of L6 cells after 2-NBDG incorporation upon stimulus by insulin (100 nM) or BQOV (25 μM). The images clearly indicate comparable glucose uptake by the cells upon treatment by the two agents. Hence, like insulin, BQOV facilitates glucose uptake in L6 myoblasts.
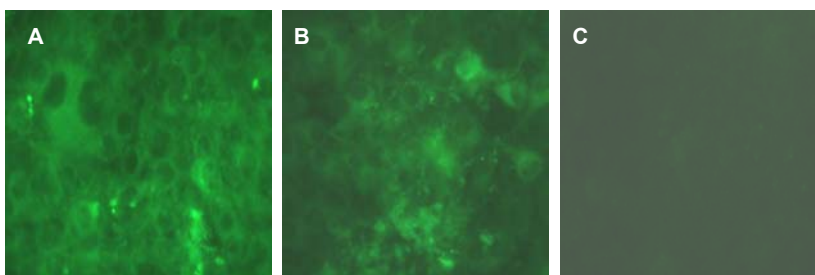

Figure 3. Glucose uptake in L6 myoblasts. 20-24 hours serum-starved L6 cells were stimulated with 100 nM insulin (**A**), 25 μM BQOV (**B**) or kept as untreated basal control (**C**) and then glucose uptake assay was performed as described in the Materials and Methods section. Cells were then observed under fluorescence microscope at 485/540 nm wavelength to observe green fluorescence of 2-NBDG.

mRNA levels of G-6-Pase and glucokinase

It was observed at the end of the study period that G-6-Pase mRNA was significantly higher, about 2.5 fold ($p < 0.05$) and glucokinase mRNA was significantly lower, about 4.8 fold ($p < 0.05$), in the livers of untreated diabetic mice as compared to normal mice. BQOV treatment normalized glucokinase and partially normalized G-6-Pase (1.7 fold) enzymes mRNA levels (Figure 4).
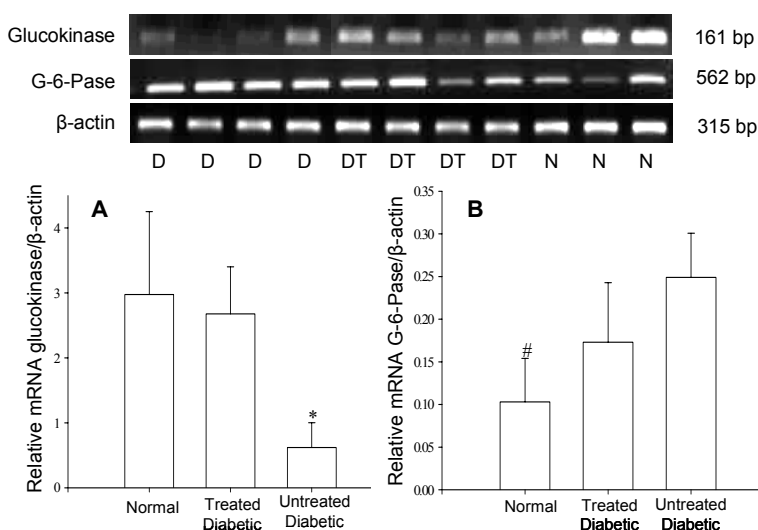
Serum antioxidant capacity

Sustained hyperglycemia had decreased free radical scavenging activity as depicted by ABTS and DPPH assays and the ferric-reducing ability of serum (FRAP value) in untreated diabetic mice. The activities were restored to normal by BQOV treatment (Table 2) indicating a reduction in overall oxidative stress.

Kidney and liver function testing

Figure 5 depicts serum analysis for urea, creatinine and alkaline phosphatase (ALP) levels. The levels were increased in untreated diabetic mice indicating kidney and liver dysfunction. However, BQOV treatment brought the urea and creatinine levels back to normal, while ALP levels were significantly reduced (125.25 ± 11.47 U/l) compared to untreated diabetic mice (161.50 ± 16.62 U/l) but remained higher than normal mice (78.00 ± 14.73 U/l), suggesting that BQOV treatment confers

Figure 4. mRNA levels of G-6-Pase and glucokinase. The graphs represent the relative mRNA of G-6-Pase (**A**) and glucokinase (**B**) with respect to β-actin in the three animal groups. Values represent mean ± SD (n = 3-5). *p < 0.05 vs. normal as well as treated diabetic animals, #p < 0.05 vs. untreated diabetic.

complete protection of the kidney and partial protection of the liver from diabetogenic insults.

Mice	FRAP QE (mg/ml serum)	ABTS Trolox eq. (mM/µl serum)	DPPH Trolox eq. (mM/ml serum)
Normal	0.15 ± 0.04	306.70 ± 15.08	12.93 ± 2.10
Diabetic (treated)	0.14 ± 0.02	284.16 ± 15.06	11.86 ± 0.66
Diabetic (untreated)	0.09 ± 0.02*	163.30 ± 13.97**	8.56 ± 0.80***

Legend: The table represents radical scavenging (ABTS and DPPH) and reducing power (FRAP) of serum of animals in the three groups at the end of the study period. Values represent mean ± SD (n = 3-5). FRAP: ferric reducing antioxidant power. QE: quercetin equivalents. ABTS: 2.2'-azinobis(3-ethylbenzothiazoline-6-sulfonic acid. DPPH: 2,2-diphenyl-picrylhydrazyl. *$p < 0.05$ vs. normal, **$p < 0.001$ vs. normal as well as treated diabetic, ***$p < 0.05$ vs. normal as well as treated diabetic.

Kidney and liver histology

The livers of untreated diabetic animals exhibited necrosis and hepatocytes with focal leukocytic infiltration were observed surrounding the injured hepatocytes. A thickening of the basement membrane of the sub-capsular glomerulus, vascular degeneration with sloughing of tubular epithelium from the basement membrane, especially from the tubules lying under the capsule, as well as protein casts in the distal convoluted tubules were observed in the kidney sections of untreated diabetic animals. However, no significant changes were observed in the liver and kidney sections of BQOV-treated diabetic animals as compared to normal animals. Thus BQOV treatment reduced the side effects of diabetes on peripheral organs.

Oxidative stress in liver and pancreas

Table 3 represents antioxidant enzyme activities (catalase, SOD and GPX), which were found to be increased in the liver and pancreas of untreated diabetic animals indicating increased oxidative stress. Similarly, there was a rise in MDA

levels (5.28 ± 0.14 and 1.89 ± 0.04 pg/mg liver and pancreas respectively) indicating increased lipid peroxidation. This oxidative stress was reduced by BQOV administration and there was significant reduction in MDA levels of both liver (4.10 ± 0.29 pg/mg) and pancreas (1.28 ± 0.04 pg/mg). However, the levels were found to be higher than those of normal mice (2.52 ± 0.03 and 1.02 ± 0.09 pg/mg in liver and pancreas respectively), which would appear to indicate the role of BQOV treatment in slowing down oxidative stress, leading to lesser tissue injury and representing a slower progression of the disease.

Pancreatic insulin content

As shown in Figure 6, normal animals exhibited >90% insulin positive cells in islets, while BQOV treated animals exhibited <10% insulin-positive cells, while the number of glucagon-positive cells increased in comparison to normal animals. However, in comparison to untreated diabetic mice, BQOV-treated islets had better morphology and more insulin-positive cells, which could be due to reduced oxidative stress. The amount of pancreatic insulin in normal animals

Table 3. Antioxidant enzyme status and oxidative stress in liver and pancreas

Mice	Liver			
	Catalase (U/mg)	SOD (U/mg)	GPX (U/mg)	MDA (pg/mg)
Normal	813.84 ± 10.04	319.56 ± 46.73	2.18 ± 0.12	2.52 ± 0.03
Diabetic (treated)	892.38 ± 0.45	296.61 ± 2.10	2.78 ± 0.03[d]	4.10 ± 0.29
Diabetic (untreated)	1267.00 ± 57.47[a]	397.76 ± 23.64[a]	3.06 ± 0.13[d]	5.28 ± 0.14[c]
	Pancreas			
	Catalase (U/mg)	SOD (U/mg)	GPX (U/mg)	MDA (pg/mg)
Normal	18.73 ± 5.62	44.10 ± 6.52	1.78 ± 0.15	1.02 ± 0.09
Diabetic (treated)	37.37 ± 7.37[c]	87.72 ± 5.64[c]	2.07 ± 0.10	1.28 ± 0.04[c]
Diabetic (untreated)	32.55 ± 0.11[c]	152.68 ± 20.51[b]	3.08 ± 0.19[e]	1.89 ± 0.04[e]

Legend: The table represents catalase, SOD and GPX enzyme activities and MDA levels in the tissues of animals in the three groups. SOD: superoxide dismutase. GPX: glutathione peroxidase. MDA: malonyldialdehydes. [a] $p < 0.05$ vs. normal and vs. treated diabetic, [b] $p < 0.05$ vs. treated diabetic, [c] $p < 0.05$ vs. normal. [d] $p < 0.001$ vs. normal, [e] $p < 0.001$ vs. normal and vs. treated diabetic.

was found to be much higher (18.04 ± 4.24 ng/mg tissue) than in the other two groups (1.20 ± 0.34 and 0.82 ± 0.15 ng/mg tissue in treated diabetic and untreated diabetic animals respectively) indicating insufficient insulin secretion even after BQOV treatment, indicating absence of pancreatic regeneration.
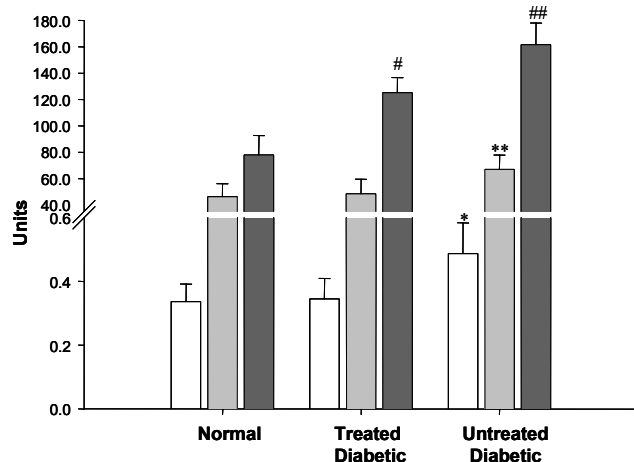

Figure 5. Serum analysis. Animal serum was analyzed for kidney and liver function. Creatinine (□) and urea (▨) was measured in mg/ml, alkaline phosphatase (▧) levels were measured in U/l. Values represent mean ± SD (n = 4-5). *p = 0.044 vs. normal, **p = 0.054 vs. normal, #p = 0.016 vs normal, ##p < 0.001 vs. normal and p = 0.003 vs. treated diabetic.

Discussion

The present investigation evaluates the effect of the recently reported organic vanadium compound, BQOV [12] on glycemic status, carbohydrate metabolism and oxidative stress in STZ-diabetic mice. Oral administration of BQOV for 3 weeks led to a reduction in blood glucose, a normalization of carbohydrate metabolism and an overall reduction in oxidative stress.

We have found a gradual reduction in random blood glucose levels and normalization of glucose tolerance (Figure 1) in STZ-diabetic mice after BQOV treatment. This is consistent with other studies, where long term vanadium treatment reduced blood glucose and normalized glucose tolerance [9]. Vanadium has been shown to increase glucose uptake by cells, whereas quercetin is known to inhibit glucose uptake by binding to the glucose binding site of GLUT4 [21]. Hence it became crucial to check the effect of BQOV treatment on the potential of the peripheral tissues for glucose uptake. An increased glucose uptake potential

in the peripheral tissues has been documented by using C[14]-2-deoxy-glucose [22], but Ball *et al.* [23] have demonstrated the validity of using fluorescent labeled glucose 2-(N-(7-nitrobenz-2-oxa-1,3-diazol-4-yl)amino)-2-deoxyglucose (2-NBDG) instead of C[14]-2-deoxy-glucose in insulin mimetic studies. Because of the ease of use of a radioactivity-free system we have used 2-NBDG as tracer glucose. 2-NDBG uptake studies (Figure 2) clearly demonstrated that the BQOV treatment has increased glucose uptake by the liver and muscles, which may account for the normal glucose tolerance observed in treated animals. The observation was further reinforced by the facilitation of glucose uptake in L6 cells by BQOV (Figure 3). This can be explained as follows: after metal complexation, quercetin, the ligand of BQOV, could no longer fit into the glucose grove of GLUT4 and thus was not able to block it.

It is known that levels of key metabolic enzymes are altered during diabetes, thus disturbing carbohydrate metabolism. Enzymes, like glucokinase, involved in glycolysis and those, like glycogen synthase, implicated in glycogen synthesis decrease while gluconeogenic enzymes, like PEPCK and G-6-Pase, increase, leading to increased hepatic output in both type 1 as well as type 2 diabetes. Vanadium compounds have been reported to normalize the levels of these enzymes [24], while quercetin is known to have no or very little effect on these enzymes levels [25, 26]. Since BQOV is a complex of vanadium and quercetin we thought it worthwhile to investigate which of these two components plays a role in restoring carbohydrate metabolism. We found that BQOV treatment normalizes mRNA levels of glucokinase and G-6-Pase in the liver (Figure 4), indicating a possible increase in glycolytic flux and a decrease in gluconeogensis, which probably results in decreased hepatic glucose output, thus decreasing random blood glucose levels in treated animals. Our studies on glucose uptake and metabolic enzyme at transcriptional levels, taken together, indicate the dominant role played by vanadium as opposed to quercetin in bringing about normalization of carbohydrate metabolism by BQOV treatment.

In addition to imbalanced carbohydrate metabolism, yet another major concern in diabetes is increased oxidative stress. Sustained hyperglycemia and increased oxidative stress are the major players in the development of secondary complications in diabetes. Quercetin is a strong antioxidant and long-term treatment of STZ-diabetic animals with quercetin has been shown to reduce oxidative stress [27] and prevent diabetic complications like nephropathy [28]. Moreover,

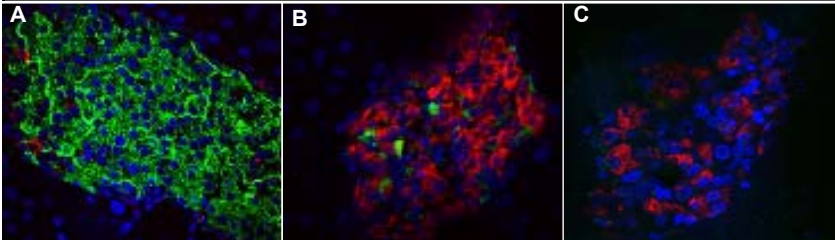| Normal	Treated Diabetic	Untreated Diabetic
18.0367± 4.24	1.2038 ± 0.34	0.8155 ± 0.15

Figure 6. Insulin level in the pancreas. The table represents the amount of insulin in pancreatic extracts of animals from different groups. Pancreatic extracts were prepared in acid-ethanol and the amount of insulin was quantitated by ELISA (ng insulin/mg pancreas). Data are mean ± SD. The pictures represent confocal images of pancreatic sections of normal (**A**), treated diabetic (**B**) and untreated diabetic (**C**) groups, where insulin is green, glucagon is red and the nucleus is stained blue by DAPI.

quercetin prevents initial tissue injury in the liver by abolishing the IKK/NF-kappaB signal transduction pathway [29]. Vanadium treatment has also been shown to have a protective effect on liver damage in streptozotocin-induced diabetic rats [30]. We have reported earlier that the metal complexation of quercetin during BQOV preparation does not hamper the antioxidant potential of quercetin [13]. Sustained hyperglycemia and increased oxidative stress are the hallmarks of diabetes, which were also observed in our untreated diabetic mice. However, BQOV treatment led to a reduction in blood glucose levels and a decrease in overall oxidative stress in the diabetic mice. Serum urea, creatinine and ALP levels indicated kidney and liver dysfunction in the untreated diabetic animals caused by increased oxidative stress, which has been ameliorated by BQOV treatment (Figure 5). Moreover, histological abnormalities caused by diabetic insults in the tissues were improved by BQOV treatment. An analysis of antioxidant status and lipid peroxidation levels in the liver and pancreas clearly revealed the protective role of BQOV (Table 3). The treatment seems to have halted further damage to the pancreas after the STZ insult, as is evident from islet morphology. This observation is consistent with the earlier report of Coskun *et al.*, where they have demonstrated that quercetin exerts a protective effect in diabetes by decreasing oxidative stress and preserving pancreatic β-cell integrity [31].

Recently, Bolkent *et al.* reported that vanadium has a protective role on β-cells and demonstrated islet regeneration upon vanadium treatment [32], while several other reports of long-term vanadium treatment claimed no increase in serum insulin levels. Similarly, contradictory reports are available for quercetin. Vessal *et al.* have reported pancreatic regeneration upon quercetin treatment [33] and other reports mention only the antioxidant potential of quercetin [27]. In order to resolve this conflicting situation we estimated the pancreatic insulin content of BQOV treated animals, which was found to be significantly lower than that of normal animals, and the number of insulin positive cells in BQOV islets was found to be much less than those in normal islets, as evidenced by immunostaining (Figure 5). However, when BQOV-treated pancreatic sections were compared with untreated ones, the number of insulin positive cells was found to be higher but insufficient to increase pancreatic insulin content to levels high enough to substantiate pancreatic regeneration. Single dose STZ insult is not likely to destroy entire β-cell mass; hence the insulin-positive cells found in BQOV-treated pancreatic sections could be residual β-cell mass leftover after STZ insult or may indicate newly formed cells, an issue which needs further investigation. Treatment of longer duration is essential to demonstrate the role of BQOV in islet neogenesis and pancreatic regeneration.

It is interesting to note that BQOV administered continuously for 3 weeks did not lead to any visible side effects like diarrhea and lethargy, which are normally associated with vanadium treatment [34] indicating quercetin's role in combating the toxic effects of vanadium. Moreover, BQOV treatment improved longevity in diabetic animals as there was about 35% mortality in the untreated diabetic group during the study period and no mortality was seen in the BQOV treatment group. Overall, our data demonstrate that BQOV represents an ideal antidiabetic compound as it retains the beneficial effects of both vanadium and quercetin and eliminates the side effects of vanadium, leading to a reduction in hyperglycemia, improvement in carbohydrate metabolism and reduction in oxidative stress, which are highly desirable in any diabetes treatment regime.

laborative work. RS wishes to thank the CSIR for providing fellowship. Special thanks are due to Dr. A.H. Hardikar for help in pancreatic sections staining and Dr. Pooja Doshi for serum antioxidant analysis testing assays.

■ References

1. **Consoli A, Nurjhan N, Capani F, Gerich J.** Predominant role of gluconeogenesis in increased hepatic glucose production in NIDDM. *Diabetes* 1989. 38:550-557.
2. **Kiss L, Szabo C.** The pathogenesis of diabetic complications: the role of DNA injury and poly(ADP-ribose) polymerase activation in peroxynitrite-mediated cytotoxicity. *Mem Inst Oswaldo Cruz* 2005. 1:29-37.
3. **Ceriello A.** Oxidative stress and diabetes-associated complications *Endocr Pract* 2006. 12(Suppl 1):60-62.
4. **Srivastava AK, Mehdi MZ.** Insulino-mimetic and anti-diabetic effects of vanadium compounds. *Diabet Med* 2005. 22:2-13.
5. **Marzban L, Rahimian R, Brownsey RW, McNeill JH.** Mechanisms by which bis(maltolato)oxovanadium(IV) normalizes phosphoenolpyruvate carboxykinase and glucose-6-phosphatase expression in streptozotocin-diabetic rats in vivo. *Endocrinology* 2002. 143:4636-4645.
6. **Mohammad A, Sharma V, McNeill JH.** Vanadium increases GLUT4 in diabetic rat skeletal muscle. *Mol Cell Biochem* 2002. 233:139-143.
7. **Srivastava AK.** Anti-diabetic and toxic effects of vanadium compounds. *Mol Cell Biochem* 2000. 206:177-182.
8. **Scior T, Guevara-Garcia A, Bernard P, Do QT, Domeyer D, Laufer S.** Are vanadium compounds drugable? Structures and effects of antidiabetic vanadium compounds: a critical review. *Mini Rev Med Chem* 2005. 5:995-1008.
9. **Yuen VG, Orvig C, McNeill JH.** Comparison of the glucose-lowering properties of vanadyl sulfate and bis(maltolato)oxovanadium(IV) following acute and chronic administration. *Can J Physiol Pharmacol* 1995. 73:55-64.
10. **Domingo JL, Gomez M, Sanchez DJ, Llobet JM, Keen CL.** Toxicology of vanadium compounds in diabetic rats: the action of chelating agents on vanadium accumulation. *Mol Cell Biochem* 1995. 153:233-240.
11. **Reul BA, Amin SS, Buchet JP, Ongemba LN, Crans DC, Brichard SM.** Effects of vanadium complexes with organic ligands on glucose metabolism: a comparison study in diabetic rats. *Br J Pharmacol* 1999. 126:467-477.
12. **Shukla R, Barve V, Padhye S, Bhonde R.** Synthesis, structural properties and insulin-enhancing potential of bis(quercetinato)oxovanadium(IV) conjugate. *Bioorg Med Chem Lett* 2004. 14:4961-4965.
13. **Shukla R, Barve V, Padhye S, Bhonde R.** Reduction of oxidative stress induced vanadium toxicity by complexing with a flavonoid, quercetin: A pragmatic therapeutic approach for diabetes. *Biometals* 2006. 19:685-693.
14. **Re R, Pellegrini N, Proteggente A, Pannala A, Yang M, Rice-Evans C.** Antioxidant activity applying an improved ABTS radical cation decolorization assay. *Free Radical Biol Med* 1999. 26:1231-1237.
15. **Arnous A, Makris DP, Kefalas P.** Effect of principle polyphenolic components in relation to antioxidant characteristics of aged red wines. *J Agri Food Chem* 2001. 49:5736-5742.
16. **Benzie IF, Strain JJ.** The ferric reducing ability of plasma (FRAP) as a measure of 'antioxidant power': The FRAP assay. *Anal Biochem* 1996. 239:70-76.

17. **Abei HE.** Catalase. In: Methods of Enzymatic Analysis. 3rd edition, Bermeyer HU, Verlagchemie GmbH, Weinhein 1993. 3:277-282.
18. **Beauchamp C, Fridovich I.** Superoxide dismutase: improved assays and an assay applicable to acrylamide gels. *Anal Biochem* 1971. 44:276-287.
19. **Lawrence RA, Burk RF.** Glutathione peroxidase activity in selenium deficient rat liver. *Biochem Biophys Res Commun* 1976. 71:952-958.
20. **Lefevre G.** Evaluation of lipid peroxidation by measuring thiobarbituric acid reactive substances. *Ann Biol Clin (Paris)* 1998. 56(3):305-319.
21. **Strobel P, Allard C, Perez-Acle T, Calderon R, Aldunate R, Leighton F.** Myricetin, quercetin and catechin-gallate inhibit glucose uptake in isolated rat adipocytes. *Biochem J* 2005. 386:471-478.
22. **Brichard SM, Desbuquois B, Girard J.** Vanadate treatment of diabetic rats reverses the impaired expression of genes involved in hepatic glucose metabolism: effects on glycolytic and gluconeogenic enzymes, and on glucose transporter GLUT2. *Mol Cell Endocrinol* 1993. 91:91-97.
23. **Ferre P, Leturque A, Burnol AF, Penicaud L, Girard J.** A method to quantify glucose utilization in vivo in skeletal muscle and white adipose tissue of the anaesthetized rat. *Biochem J* 1985. 228:103-110.
24. **Ball SW, Bailey JR, Stewart JM, Vogels CM, Westcott SA.** A fluorescent compound for glucose uptake measurements in isolated rat cardiomyocytes. *Can J Physiol Pharmacol* 2002. 80:205-209.
25. **Koyama Y, Abe K, Sano Y, Ishizaki Y, Njelekela M, Shoji Y, Hara Y, Isemura M.** Effects of green tea on gene expression of hepatic gluconeogenic enzymes in vivo. *Planta Med* 2004. 70:1100-1102.
26. **Estrada O, Hasegawa M, Gonzalez-Mujica F, Motta N, Perdomo E, Solorzano A, Mendez J, Mendez B, Zea EG.** Evaluation of flavonoids from Bauhinia megalandra leaves as inhibitors of glucose-6-phosphatase system *Phytother Res* 2005. 19:859-863.
27. **Mahesh T, Menon VP.** Quercetin alleviates oxidative stress in streptozotocin-induced diabetic rats. *Phytother Res* 2004. 18:123-127.
28. **Anjaneyulu M, Chopra K.** Quercetin, an anti-oxidant bioflavonoid, attenuates diabetic nephropathy in rats. *Clin Exp Pharmacol Physiol* 2004. 31:244-248.
29. **Dias AS, Porawski M, Alonso M, Marroni N, Collado PS, Gonzalez-Gallego J.** Quercetin decreases oxidative stress, NF-kappaB activation, and iNOS overexpression in liver of streptozotocin-induced diabetic rats. *J Nutr* 2005. 135:2299-2304.
30. **Koyuturk M, Tunali S, Bolkent S, Yanardag R.** Effects of vanadyl sulfate on liver of streptozotocin-induced diabetic rats. *Boil Trace Elem Res* 2005. 104:233-247.
31. **Coskun O, Kanter M, Korkmaz A, Oter S.** Quercetin, a flavonoid antioxidant, prevents and protects streptozotocin-induced oxidative stress and beta-cell damage in rat pancreas. *Pharmacol Res* 2005. 51:117-123.
32. **Bolkent S, Bolkent S, Yanardag R, Tunali S.** Protective effect of vanadyl sulfate on the pancreas of streptozotocin-

induced diabetic rats. *Diabetes Res Clin Pract* 2005. 70:103-109.

33. **Vessal M, Hemmati M, Vasei M.** Antidiabetic effects of quercetin in streptozocin-induced diabetic rats. *Comp Biochem Physiol C Toxicol Pharmacol* 2003. 135C(3):357-364.

34. **Majithiya JB, Balaraman R, Giridhar R, Yadav MR.** Effect of bis[curcumino]oxovanadium complex on non-diabetic and streptozotocin-induced diabetic rats. *J Trace Elem Med Biol* 2005. 18:211-217.